

# Measurements and data-based predictions for $\Delta n = 1$ resonance and intercombination transitions in the Be and Ne sequences

L. J. Curtis, S. T. Maniak, R. W. Ghrist, R. E. Irving, D. G. Ellis,  
M. Henderson, and M. H. Kacher

*Department of Physics and Astronomy, University of Toledo, Toledo, Ohio 43606*

E. Träbert and J. Granzow

*Experimentalphysik III, Ruhr-Universität Bochum, D-44780 Bochum, Germany*

P. Bengtsson and L. Engström

*Fysiska Institutionen, Lunds Universitet, S-223 62 Lund, Sweden*

(Received 12 December 1994)

Earlier studies of line strengths for  $ns^2\ ^1S_0$ - $nsn'p\ ^1,3P_1$  resonance and intercombination transitions for intrashell ( $n'=n$ ) cases have revealed isoelectronic regularities that have been used to make accurate predictions along the sequence. Although lifetime data exist for intershell ( $n' > n$ ) cases, the lack of branching ratio measurements has until now prevented similar analyses. Through new lifetime measurements, a critical evaluation of the available data, and determinations of branching fractions from a differential measurement and from calculational considerations, we have extended these methods to systematize and predict line strengths for  $\Delta n=1$  resonance and intercombination transitions in the Be and Ne sequences.

PACS number(s): 32.70.-n

## I. INTRODUCTION

Many experimental studies exist for the intrashell line strengths of the  $ns^2\ ^1S_0$ - $nsn'p\ ^1,3P_1$  resonance and intercombination lines in the spectra of ions of the alkaline-earth-atom-like isoelectronic sequences. For these  $\Delta n = 0$  transitions in closed core systems such as the Be, Mg, and Zn sequences, experimental determination of line strengths can be made directly from lifetime measurements, since  $nsnp$  is the first excited configuration, and there is only the single decay branch to the ground state. This is in sharp contrast to the situation for the intershell transitions of the form  $ns^2\ ^1S_0$ - $nsn'p\ ^1,3P_1$  with  $n' \neq n$ , for which other decay branches (e.g., to  $nsn's$  and  $np^2$  levels) compete. Thus, although a similar (but smaller) base of experimental lifetime data exists for these transitions, it is not possible to convert these data to oscillator strengths and line strengths, since virtually *no* branching ratio information is available for charged ions in *any* sequence.

This is unfortunate, because interesting isoelectronic trends have been observed for the  $\Delta n = 0$  transitions of this type. For example, a data-based method has been developed [1-5] in which the singlet-triplet mixing amplitudes are characterized from spectroscopic energy level data as a mixing angle, which can be used to place both the resonance and the intercombination line strengths in a common graphical exposition. This exposition reveals common isoelectronic regularities that permit the resonance transition data (usually measurable only for low to medium degrees of ionization) to be combined with the intercombination transition data (usually measurable only for medium to high degrees of ionization).

It would be useful to explore whether these trends persist for  $\Delta n \geq 1$ , if a source of experimental data were available.

One counterexample and one counteranalog to the dearth of  $\Delta n \geq 1$  line strength data exist. The counterexample concerns the  $2s^2\ ^1S_0$ - $2s3p\ ^1,3P_1$  transitions in the Be isoelectronic sequence. Here differential lifetime measurements in the  $2s3s\ ^3S_1$ - $2s3p\ ^3P_{2,1,0}$  decay channels reveal the branch to the ground state as an extra channel available only to the  $^3P_1$  level. Moreover, the  $^1P_1$  level decays dominantly to the ground state and other branching can be estimated theoretically without large error. The counteranalog involves the  $2p^6\ ^1S_0$ - $2p^53s\ ^1,3P_1$  transitions in the Ne sequence, for which the first excited state is extrashell, giving rise to unbranched  $\Delta n = 1$  resonance and intercombination transitions. Despite the obvious differences in their structures, striking similarities exist between these two systems. We shall show that these two transitions in different sequences are in some ways more closely related to each other than to other transitions within their own sequence.

We present here an experimental study that reports new lifetime measurements for  $\Delta n = 1$  resonance and intercombination transitions in these Be and Ne isoelectronic sequences and combines them with a critical evaluation of earlier measurements and a predictive parametrization of the data base formed.

## II. EXPOSITION OF LIFETIME DATA AS REDUCED LINE STRENGTHS

The standard line strength factor  $S_{if}$  for a transition from an upper level  $i$  to a lower level  $f$  is obtained from

the transition probability rate  $A_{if}$  and the transition wavelength  $\lambda_{if}$  with the relationship

$$S_{if} = [\lambda_{if}(\text{\AA})/1265.38]^3 g_i A_{if} (\text{ns}^{-1}), \quad (1)$$

where  $g_i = 3$  is the degeneracy for an upper state with  $J = 1$ . The transition probability can be obtained from the measured lifetime  $\tau_i$  either from a knowledge of the branching fraction  $B_{if}$

$$A_{if} = B_{if}/\tau_i \quad (2)$$

( $B_{if} = 1$  for an unbranched transition) or from the difference between the lifetimes of two fine structure levels of the same  $LS$  term that differ only by the presence of an additional channel, which (neglecting small differences in wavelength factors within the fine structure manifold) yields

$$A_{if} = 1/\tau_i(J_1) - 1/\tau_i(J_2). \quad (3)$$

For a two-electron or an electron-hole system that has a predominantly  $sp$  configurational character, an effective singlet-triplet mixing angle can be defined from the measured energy levels (represented here by their spectroscopic symbols in  $LS$  coupling notation) as [1]

$$\cot(2\vartheta) \equiv \pm \frac{1}{\sqrt{2}} \left[ \frac{3(^3P_1 + ^1P_1 - 2^3P_0)}{2(^3P_2 - ^3P_0)} - 1 \right]. \quad (4)$$

Because of its empirical nature, this quantity will implicitly contain the effects of configuration interaction, but it can nonetheless be used to convert the measured line strengths for the (nominally) spin-allowed resonance line  $S_{if}(\text{res})$  and the spin-forbidden intercombination line  $S_{if}(\text{int})$  to "reduced line strength" values  $S_{if}^r(\text{res})$  and  $S_{if}^r(\text{int})$ , defined as [1]

$$S_{if}^r(\text{res}) \equiv S_{if}(\text{res})/\cos^2 \vartheta, \quad (5)$$

$$S_{if}^r(\text{int}) \equiv S_{if}(\text{int})/\sin^2 \vartheta. \quad (6)$$

In the single-configuration limit, these reduced line strengths would be proportional to the squared radial dipole matrix elements for the two transitions and, provided there are no strong cancellation effects [6], they should have similar slowly varying isoelectronic behaviors. The presence of a configuration interaction will complicate only the physical interpretation, and not the expository utility of this parametrization, provided the effective reduced line strengths exhibit isoelectronic regularity. This parametrization can be particularly valuable in cases where the configuration interaction is indirect, perturbing the singlet-triplet mixing but not contributing a significant configuration state amplitude to the overall wave function.

It has been found [1-5] that the isoelectronic behavior of the reduced line strengths often can be accurately represented by

$$Z^2 S^r \cong a + b/(Z - c). \quad (7)$$

Experimental data are usually more extensively and more accurately available for the lower members of an isoelectronic sequence. Since interpolations are more reliable than extrapolations, it would be very useful if an asymptotic value for  $Z^2 S$  at high  $Z$  could be established to permit predictive use of Eq. (7). For high- $Z$  members of an isoelectronic sequence it would be expected that the interaction of the active electron with the central nuclear charge would dominate over the interactions with the individual electrons and that the line strength would approximate that of a hydrogenlike system. In the nonrelativistic Schrödinger approximation, the  $Z^2$ -scaled line strengths are independent of  $Z$  and, for the  $n=2-3$  shell,  $\ell=0-1$  subshell transitions considered here, are given (for the  $J=\frac{1}{2}-\frac{1}{2}$  transitions) by

$$Z^2 S_{2s,3p} = 2^{21} 3^6 / 5^{12} = 6.26206\dots, \quad (8)$$

$$Z^2 S_{2p,3s} = 2^{16} 3^7 / 5^{12} = 0.587068\dots \quad (9)$$

(For the  $J=\frac{1}{2}-\frac{3}{2}$  transitions the values are larger by a factor 2.) For very high- $Z$  charge states, calculations of the relativistic corrections have been obtained [7,8] from the corresponding solution of the Dirac equation, but the nonrelativistic approximation should be sufficient for the range of the empirical trends studied here.

In taking the high- $Z$  limit of a two-electron system, attention must be given to the fact that the even parity  $n=2$  complex ( $K^2 L^2$ ) mixes  $2s^2$  and  $2p^2$  and the odd parity  $n=3$  complex ( $K^2 LM$ ) mixes  $2s3p$ ,  $2p3s$ , and  $2p3d$ . To investigate this mixing in the high- $Z$  limit, we use  $1/Z$  perturbation theory. The sum of all the two-electron interactions is treated as a perturbation, with the unperturbed states being represented by products of Dirac hydrogenic wave functions, using  $jj$  coupling. To get the correct zeroth-order (high- $Z$ ) mixing, we need only consider states that are degenerate with respect to the Dirac-Sommerfeld energies. For these cases we can diagonalize the interaction matrix and compute the mixing amplitudes. We have done this calculation nonrelativistically and estimated the relativistic corrections.

For the case of the Be sequence, we find that the mixing is too small to be important for the present analysis, namely, 2.65% for  $2s^2-2p^2$ , 0.73% for  $2s3p-2p3s$ , and 0.08% for  $2s3p-2p3d$ . A similar calculation using an  $LS$  rather than a  $jj$  basis set has been made by Linderberg and Shull [9]. As expected, the mixing in the  $LS$  basis was slightly larger and yielded approximately 5% for  $2s^2-2p^2$ . For the case of the Ne sequence, this kind of high- $Z$  analysis is not yet appropriate because the available data are so far from that limit. As  $Z$  increases to 40 and above, the  $2p^5 3s$   $J=1$  levels must negotiate a series of crossings with levels from the  $2p^5 3d$  configuration, none of which gives rise to an asymptotic degeneracy. Only then can a high- $Z$  degeneracy with  $2s2p^6 3p$  be approached.

Therefore we find that the proper limiting values for the line strengths considered here are simply obtained from the one-electron case, via appropriate angular momentum combinations, assuming no zeroth-order mixing. The results are just those given in Eqs. (8) and (9) multiplied by a factor of 3,

$$Z^2 S_{2s^2, 2s3p} = 3(6.26206\dots) = 18.7862\dots, \quad (10)$$

$$Z^2 S_{2p^6, 2p^53s} = 3(0.587068\dots) = 1.76121\dots \quad (11)$$

### III. EXPERIMENT

In order to obtain appropriate conditions of beam energy and spectroscopic wavelength range, the beam-foil excited decay curve measurements were made in three different accelerator laboratories. The measurements on C and Ne were performed using the 330-kV Danfysik Heavy Ion Accelerator at the University of Toledo with a normal incidence vacuum ultraviolet monochromator; measurements on N, O, F, Na, Mg, Al, Si, and P were performed using the 400-kV Sames single stage and the 4-MV Dynamitron Tandem accelerators at the University of Bochum with a grazing incidence extreme ultraviolet monochromator, and additional measurements on F were performed using the 3-MV Tandem Pelletron accelerator at the University of Lund with a normal incidence monochromator. These facilities and the details of the experimental techniques used have been described elsewhere [10–14]. The desired ions were produced by the appropriate accelerator, momentum analyzed, and directed through a thin self-supporting carbon foil. The light emitted by the foil-excited ions was analyzed with a monochromator appropriate to the spectral region under study. The decay curves were measured by recording the intensity of the spectral lines as a function of the distance from the foil. The decay curves were analyzed by multiexponential curve fitting techniques, assisted by simulations of cascade repopulation.

### IV. COMPARISON OF THE TWO SEQUENCES

Superficially, the  $2s^2$ - $2s3p$  transitions in the Be sequence and the  $2p^6$ - $2p^53s$  transitions in the Ne sequence seem to have little in common aside from their  $LS$  angular momentum scheme  $^1S_0$ - $^3P_J$ . The two-electron and the electron-hole aspects cause the configurations in the complexes to be quite different and intermediate coupling joins the  $LS$  and the  $jj$  limits in different ways. [For the Be  $2s3p$  case  $^1P_1$  and  $^3P_2$  correspond to  $(\frac{1}{2}, \frac{3}{2})$  and  $^3P_1$  and  $^3P_0$  correspond to  $(\frac{1}{2}, \frac{1}{2})$ ; for the Ne  $2p^53s$  case  $^1P_1$  and  $^3P_0$  correspond to  $(\frac{1}{2}, \frac{1}{2})$  and  $^3P_1$  and  $^3P_2$  correspond to  $(\frac{1}{2}, \frac{3}{2})$ .] However, similarities emerge when one considers the isoelectronic behavior of the mixing of the  $J=1$  singlet and triplet levels as characterized by the mixing angle as defined in Eq. (4). The mixing angles for these two configurations have been computed from available spectroscopic data (as described below) and a plot of their  $\sin^2$  vs the nuclear charge is given in Fig. 1. For comparison purposes, a plot of the corresponding quantity for the  $2s2p$  transitions in the Be sequence is also plotted.

Note that, unlike the case for the  $2s2p$  sequence, both

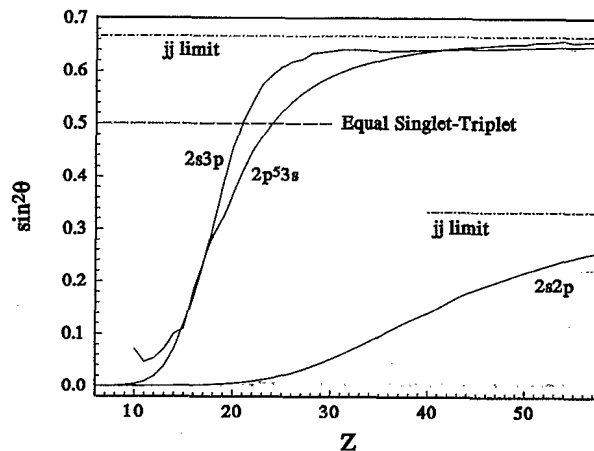


FIG. 1. Plot of the mixing angles for  $J=1$  levels of the  $2s2p$  and the  $2s3p$  configurations in the Be sequence and the  $2p^53s$  configuration in the Ne sequence vs the nuclear charge.

the  $2s3p$  and the  $2p^53s$  configurations pass through a value of  $45^\circ$  for the mixing angle, where the singlet and the triplet amplitudes reverse their roles as the dominant amplitude in the wave function. Although the energy levels are quite widely separated, this nonetheless corresponds to an *avoided crossing* in energy, which is a true *crossing* of the eigenvectors. As has been discussed elsewhere [15,16], it is necessary to trace the crossing of eigenvectors and not the avoided crossing of energy levels to obtain isoelectronic regularity. As can be seen from Fig. 1, the reversal of singlet and triplet content occurs in the Be  $2s3p$  sequence at  $Z \cong 21$  and in the Ne  $2p^53s$  sequence at  $Z \cong 24$ . Clearly, for purposes of this mixing angle formulation, the behavior of the Be  $2s^2$ - $2s3p$  sequence is much more closely related to the Ne  $2p^6$ - $2p^53s$  than to the Be  $2s^2$ - $2s2p$ .

Another similarity exists at the beginning of the two sequences. As has been noted earlier [17], because of the configuration interaction (with, e.g.,  $2p3s$ ), the Be  $2s3p$  configuration has another avoided crossing between  $Z=5$  and 6, which can cause notational confusion. Here the spectroscopic references label the lowest  $J=1$  level as a triplet for  $Z=4$ –5 [18,19] and as a singlet for  $Z=5$ –9 [20–24]. Thus the avoided crossing at  $Z=21$  occurs from a notational labeling that is opposite Hund's rule. Another unusual effect occurs near the neutral end of the sequence of the Ne  $2p^53s$  configuration. As can be seen from Fig. 1, the mixing angle for Ne I is larger than that of either Na II or Mg III, an effect that occurs in conjunction with a strong contraction of the  $3s$  orbital that occurs between Ne I and Na II [16]. As will be discussed later, these conditions require special care in the application of the mixing angle methods at the extreme neutral end of these sequences.

### V. BERYLLIUM SEQUENCE

We have previously applied the mixing angle formulation to a study of the resonance and intercombina-

tion lines of the  $2s^2-2s3p$  transitions in the Be isoelectronic sequence [17]. These intershell transitions provide a stringent test of the method since they introduce complications from interactions with plunging configurations, transition integral cancellations, and multiple exit channels, which were not present in the case of the intrashell transitions.

### A. Data sources

The mixing angle and wavelength values were determined from experimental and calculational sources. Complete spectroscopic energy level data are available for the elements Be I-Ne VII [18-24]. These were supplemented for the higher ionization stages by the theoretical calculations of energy levels by Ellis [25], and of wavelengths and mixing angles (deduced from line strength ratios) by Kim *et al.* [26].

The intercombination transition probability data are available for this particular system because of an experimental technique that has been developed [27] for this purpose. This involves the fine structure resolved measurement of the lifetimes of the  $^3P_J$  for  $J=0,1,2$  in an allowed branch, such as  $2s3s^3S_1-2s3p^3P_J$ . The lifetimes of the  $J=0$  and 2 levels are essentially equal, but the  $J=1$  is shortened by the additional relativistic  $E1$  channel to the ground state that is available only to it. The  $2s^2^1S_0-2s3p^3P_1$  transition probability is obtained either by subtracting the fitted lifetimes or by fitting the logarithmic ratio of the decay curves. Measurements for this transition have been reported in the literature for N IV, O V, F VI [27], Ne VII [28], Na VIII, Mg IX, Al X, and Si XI [29]. Of these, the data on N through Ne were obtained using the above method dealing with spectrally resolved lines. The data for Na through Si were obtained from the unresolved multiplet  $2p^2^3P-2s3p^3P^o$  and consequently suffer from the problems of evaluating complex decay curves. The F VI measurement [27] exhibited inconsistencies with the trend of the measurements, so we performed new measurements, which we report here. A number of theoretical studies of this system have also been reported [25,26,30-33].

Earlier lifetime measurements for the resonance line have been made for B II [34-36], C III [37], N IV [38], and O V [39]. We have supplemented these results with our

TABLE I. Theoretical branching fractions (in percent). Fe values are from Ref. [41] and the other values are from Ref. [40].

$2s3p^1P_1$	$2s^2^1S_0$	$2p^2^1D_2$	$2p^2^1S_0$	$2s3s^1S_0$
Be I	55.6	26.5	0.1	17.9
B II	68.6	14.4	13.9	3.0
C III	87.3	11.6	0.8	0.25
N IV	89.9	9.5	0.4	0.10
O V	91.4	8.2	0.3	0.05
Ne VII	93.5	6.3	0.2	0.02
Fe XXIII	95.9	3.1	0.1	

own remeasurements in C III, N IV, and O V, and added a new measurement for F VI. In order to convert these lifetimes to transition probabilities, we have obtained estimates of branching fractions using published theoretical calculations of oscillator strengths. Values for  $Z=4-8,10$  were taken from the calculations of Laughlin *et al.* [40], which were interpolated to the calculation of Bhatia and Mason [41] for  $Z=26$ . The branching fractions for the  $2s3p^1P_1$  decay to the  $2s^2$ ,  $2s3s$ ,  $2p^2^1S_0$  levels and to the  $2p^2^1D_2$  level are given in Table I. These indicate that the decay is branched by 87% to the ground state already for C III, and by more than 90% for higher degrees of ionization. We therefore assume that the uncertainty introduced by the use of the theoretical branching fractions is smaller than the uncertainties in the lifetime measurements.

Experimental values for the fine structure resolved triplet lifetimes, the singlet lifetime, and the computed and the interpolated branching ratios are listed in Table II. Note that a misprint in Ref. [29] that occurred for Na VIII has been corrected in Table II.

### B. Results

The triplet lifetimes and their reciprocal differences and the singlet lifetimes and their branching ratios are given in Table II. Our new measurements for the F VI triplet yielded a reciprocal lifetime difference of  $0.102 \pm 0.009 \mu s^{-1}$ , which supersedes the value  $0.088 \pm 0.008 \mu s^{-1}$  reported earlier in Ref. [27]. Our new measurements for the singlets yielded lifetimes of  $280 \pm 40$  ps for C III,  $87 \pm 5$  ps for N IV,  $41 \pm 4$  ps for O V, and  $24 \pm 4$  ps for F VI. A plot of scaled reduced line strengths  $Z^2 S^r(\text{res})$  and  $Z^2 S^r(\text{int})$  vs the reciprocal screened charge is displayed in Fig. 2. Separate weighted least-squares fits have been made for each, constrained to

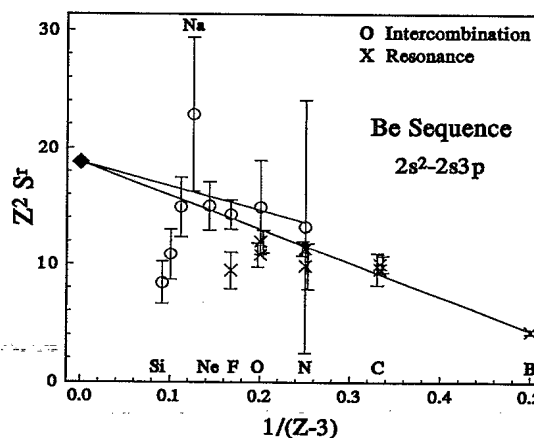


FIG. 2. Plot of the charge-scaled reduced line strengths vs the reciprocal screened charge for the  $2s^2-2s3p$  transitions in the Be isoelectronic sequence. Measured values are denoted by  $\circ$  for the intercombination transition and by  $\times$  for the resonance transition. The high- $Z$  hydrogenlike limit is denoted by  $\diamond$  and the solid lines trace weighted least-squares fits.

TABLE II. Be sequence  $2s3p^{1,3}P$  levels (lifetimes in ns). The experimental uncertainty in the last figure is given in parentheses. Branching fractions without labels are interpolated.

$Z$	Ion	Intercombination transitions				Resonance transitions				$\sin \theta$
		$\tau_{2,0}$	$\tau_1$	$A_{\text{expt}}$	$A_{\text{pred}}$	$\tau$	$BF$	$A_{\text{expt}}$	$A_{\text{pred}}$	
5	B				0.0001	1.98(9) <sup>a</sup>	0.686 <sup>b</sup>	0.346(16)	0.35	0.0199
6	C				0.0004	0.28(4) <sup>c</sup>	0.873 <sup>b</sup>	3.12(45)	2.95	0.0113
						0.268(20) <sup>d</sup>		3.26(24)		
7	N	8.98(10)	8.72(12)	0.0033(20) <sup>e</sup>	0.0028	0.087(5) <sup>c</sup>	0.899 <sup>b</sup>	10.3(6)	10.4	0.0164
						0.10(2) <sup>f</sup>		9(2)		
8	O	5.31(5)	4.74(7)	0.0226(4) <sup>e</sup>	0.019	0.041(4) <sup>c</sup>	0.914 <sup>b</sup>	22(2)	26.5	0.0266
						0.037(3) <sup>g</sup>		25(2)		
						0.024(4) <sup>c</sup>	0.927	39(6)	56.2	0.0419
9	F	2.94(3)	2.24(4)	0.102(9) <sup>e</sup>	0.100				105	0.0627
10	Ne	1.75(7)	1.00(6)	0.43(6) <sup>h</sup>	0.418		0.934 <sup>b</sup>		180	0.0959
11	Na	1.10(16)	0.29(6)	2.54(73) <sup>i</sup>	1.68		0.939		286	0.1400
12	Mg	0.745(60)	0.145(20)	5.55(96) <sup>i</sup>	5.76		0.943		429	0.1980
13	Al	0.515(50)	0.071(12)	12.1(24) <sup>i</sup>	17.6		0.946		609	0.2688
14	Si	0.365(25)	0.036(7)	25.0(54) <sup>i</sup>	47.7		0.949		822	0.3441
15	P				111		0.951		1065	0.4155
16	S				223		0.952		1327	0.4851
17	Cl				410		0.953		1584	0.5558
18	Ar				711		0.955		1828	0.6209
19	K				1153		0.955		2079	0.6732
20	Ca				1732		0.956		2375	0.7098
21	Sc				2426		0.957		2749	0.7360
22	Ti				3226		0.957		3151	0.7574
23	V				4207		0.958		3835	0.7699
24	Cr				5130		0.958		4435	0.7792
25	Mn				6393		0.959		5130	0.7859
26	Fe				7850		0.959 <sup>j</sup>			

<sup>a</sup>Kernahan *et al.*, Ref. [57].

<sup>b</sup>Laughlin *et al.*, Ref. [40].

<sup>c</sup>This work.

<sup>d</sup>Buchet-Poulizac and Buchet, Ref. [37].

<sup>e</sup>Engström *et al.*, Ref. [27].

<sup>f</sup>Dumont *et al.*, Ref. [38].

<sup>g</sup>Knystautas and Drouin, Ref. [39].

<sup>h</sup>Hardis *et al.*, Ref. [28].

<sup>i</sup>Granzow *et al.*, Ref. [29].

<sup>j</sup>Bhatia and Mason, Ref. [41].

intersect the high- $Z$  asymptotic value of 18.786. The predictions made from these fits are also given in Table II. It is clear from Fig. 2 that the trend of the measurements for the intercombination transitions for Na VIII, Al X, and Si XI [29] (see comment above) is contrary to the general trend and additional experimental studies of these systems should certainly be made.

## VI. NEON SEQUENCE

The  $2p^6-2p^53s$  resonance and intercombination transitions in the Ne isoelectronic sequence are unbranched and their measured lifetimes can be used directly in the mixing angle reduction approach [42]. The intershell nature of these  $\Delta n=1$  inert-gas-like transitions causes them to have substantially shorter wavelengths (and hence shorter lifetimes) than those that characterize the corresponding unbranched  $\Delta n=0$   $ns^2-nsp$  transitions in alkaline-earthlike systems. These shorter lifetimes severely limit the members of the sequence that are accessible to measurement and motivate the use of data-based methods for their reliable prediction.

These transitions are particularly interesting because

it is possible to create a population inversion between the  $2p^53s$  and the  $2p^53p$  levels that can produce soft x-ray laser amplification. Modeling studies have demonstrated that amplification is optimal near  $Z=36$ , leading to tests at  $Z=34$  and  $Z=39$  in Se [43] and Y [44] plasmas. Although the lifetimes of these levels are too short for time-of-flight measurements in the vicinity of  $Z=36$ , the mixing angle formulation and the high- $Z$  asymptote permit interpolation of trends if precision results at lower  $Z$  are available.

### A. Data sources

Critical compilations of spectroscopic energy level data for the Ne sequence are available for Ne I–Si V [45,46] and classification work is available for P VI–K X [47–51]. Additional data are available from laser-produced plasmas for Ca XI–Mn XVI [52] and from beam foil studies for Fe XVII–Cu XX [53]. These can be coupled with theoretical studies that cover the regions  $Z=16-80$  [54] and  $Z=28-92$  [55].

A number of experimental measurements of the  $2p^53s^{1,3}P_1$  lifetimes have been reported [56–63], for which we have made a critical evaluation. High precision

measurements of the resonance and intercombination lifetimes have been made for Ne-like S VII and Cl VIII [61]. These studies yielded lifetimes with quoted uncertainties of up to 3–4%, a substantial improvement over earlier measurements for these ions [62,63], which had uncertainties exceeding 25%. Reference [61] used a specially designed beam-foil chamber [14] that views a very short segment of beam with a grazing incidence monochromator, permitting precision measurement of picosecond lifetimes. Lifetimes were extracted using the method of correlated analyses of decay curves (ANDC) [64], which incorporates the decay curves of both the primary  $2p^6-2p^53s$  transitions and the dominant cascade  $2p^53s-2p^53p$  into the analysis. Subsequent to the publication of Ref. [61], an extension of that study of S VII was undertaken [65] to investigate discrepancies between theoretical [66] and experimental [67] results for the  $3d$  lifetimes. In addition to remeasurements of the  $3s-3p-3d$  decays, this study provided new measurements of the decays of the higher-lying  $4p$ ,  $4f$ , and  $5g$  levels, which make possible coupled ANDC [68] along the cascade chain. These studies in S VII have confirmed the value for the lifetime of the  $2p^53s^3P_1$  level to be  $52\pm 2$  ps (as reported in Ref. [61]), but indicates a revised value for the lifetime of the  $2p^53s^1P_1$  level of  $14.5\pm 1.0$  ps, which supersedes the value  $17.4\pm 0.5$  ps that was reported in Ref. [61]).

For Ne I there is an inconsistency between the two previously reported measurements [56,57], which we sought

to resolve through new measurements. Earlier measurements for Na II [58] and for Ar IX [63] are not sufficiently accurate to establish isoelectronic trends. (The quoted uncertainty of 0.5% for the Na II intercombination lifetime in Ref. [58] is quoted elsewhere [59] as 5%, and is clearly a misprint.) Reasonably accurate measurements are available for Mg III [60]. We have performed new measurements in the ions Ne I–P VI, and have sought, through a combination of these and earlier measurements [56–61,65,62,63], to establish predictive trends.

## B. Results

A summary of the lifetime data is given in Table III. Our new measurements for the singlet lifetimes yielded  $1470\pm 100$  ps for Ne I,  $320^{+50}_{-40}$  ps for Na II,  $110^{+15}_{-10}$  ps for Mg III,  $46^{+10}_{-5}$  ps for Al IV, and  $18^{+7}_{-2}$  ps for P VI. Our new measurements for the triplet lifetimes yielded  $29.6\pm 1.0$  ns for Ne I,  $6.0\pm 1.2$  ns for Na II, and  $130\pm 30$  ps for P VI. The measurements yielded decay curves that, by virtue of good time resolution and sufficient signal statistics, gave evidence for severe problems to be dealt with in the data evaluation. These problems result from the manifold of  $n=3$ ,  $\Delta n=0$  cascade transitions feeding the levels of interest, with secondary repopulation that causes both the primary and the cascade decay curves to exhibit a

TABLE III. Ne sequence  $2p^53s^1,3P$  levels (lifetimes in ps).

$Z$	Ion	Intercombination transitions		Resonance transitions		$\sin \theta$
		$\tau_{\text{expt}}$	$\tau_{\text{pred}}$	$\tau_{\text{expt}}$	$\tau_{\text{pred}}$	
10	Ne	$29600\pm 1000, 10^{\text{a},\text{j}}$		$1470\pm 100^{\text{a}}$	1547	0.2656
		$31700\pm 1600, 10^{\text{b},\text{j}}$		$1870\pm 180, 10^{\text{b},\text{j}}$		
		$29800\pm 2000, 10^{\text{c},\text{j}}$		$1300\pm 100, 10^{\text{c},\text{j}}$		
11	Na	$6000\pm 1200^{\text{a}}$	5623	$320^{+50}_{-40}$	346	0.2131
		$10600\pm 500, 10^{\text{d},\text{j}}$		$580\pm 60^{\text{d}}$		
12	Mg	$1900\pm 190^{\text{e}}$	1820	$100\pm 15^{\text{e}}$	131	0.2299
13	Al		637	$110^{+15}_{-10}$		0.2677
				$46^{+10}_{-5}$	63	
14	Si		248	$28^{+8}_{-4}$	36	0.3171
15	P	$130\pm 30^{\text{a}}$	137	$18^{+7}_{-2}$	21	0.3731
16	S	$52\pm 2^{\text{f}}$	52	$14.5\pm 1.0^{\text{g}}$	15	0.4309
		$49\pm 13^{\text{h},\text{j}}$		$12\pm 3^{\text{h},\text{j}}$		
17	Cl	$27\pm 1^{\text{f}}$	27	$13\pm 1^{\text{f}}$	11	0.4872
		$34\pm 12^{\text{h},\text{j}}$		$10\pm 2^{\text{h},\text{j}}$		
		$30\pm 5^{\text{i},\text{j}}$		$8\pm 2^{\text{i},\text{j}}$		
18	Ar	$19\pm 4^{\text{i},\text{j}}$	16	$6.5\pm 2.0^{\text{i},\text{j}}$		
34	Se		0.28		0.60	0.7847
35	Br		0.24		0.53	0.7878
36	Kr		0.21		0.47	0.7904
37	Rb		0.19		0.42	0.7927
38	Sr		0.16		0.38	0.7947
39	Y		0.14		0.34	0.7966

<sup>a</sup>This work.

<sup>b</sup>Lawrence and Liszt, Ref. [56].

<sup>c</sup>Kernahan *et al.*, Ref. [57].

<sup>d</sup>Schlagheck, Refs. [58,59].

<sup>e</sup>Buchet *et al.*, Ref. [60].

<sup>f</sup>Westerlind *et al.*, Ref. [61].

<sup>g</sup>Kirm *et al.*, Ref. [65].

<sup>h</sup>Gardner *et al.*, Ref. [62].

<sup>i</sup>Berry *et al.*, Ref. [63].

<sup>j</sup>Excluded from plot and fit.

heavy growing-in pattern. This can cause systematic errors in standard multiexponential fits to the triplet decay data, and degrade the reliability of lifetimes determined from the triplet level decay curve alone. A solution of this problem would require the measurement of the decay curves of the complete set of cascade levels, which were not accessible in this experiment.

A reduction of these data to values for  $S^r(\text{res})$  and  $S^r(\text{int})$  is plotted vs  $1/(Z-8)$  in Fig. 3. In this case the high- $Z$  asymptotic value is 1.761. Weighted least-squares fits for this reduced data for the resonance and intercombination transitions are indicated by the solid lines. Predicted lifetimes obtained from these fits are given in Table III. These linear interpolations yield lifetimes for the resonance and intercombination lines of 0.60 ps and 0.28 ps for  $\text{Se}^{24+}$  and 0.34 ps and 0.14 ps for  $\text{Y}^{29+}$ . (The reversed ordering of lifetimes occurs because of the avoided crossing at  $Z=21$ . As discussed earlier, isoelectronic smoothness requires that this be treated as though it were a crossing [15].) Although these lifetime measurements are not of sufficient accuracy and breadth to confirm the validity of the linearity expressed in Eq. (7), the isoelectronic trend is clearly regular and slowly varying. Significant discrepancies exist among *ab initio* calculations [55,69-73], which this semiempirical work can help to clarify. As additional measurements of lifetimes in low to moderate members of this sequence become available, the predictions for ions at higher  $Z$  (which have immeasurably short lifetimes) could be sharpened. If this semiempirical approach proves to be extrapolatively reliable to a degree commensurate with the 3-4% accuracies provided by some of the measurements, these estimates could be valuable for plasma modeling purposes.

The intercombination transition for  $\text{Ne I}$  was not included in the fitting process, because there are reasons to believe that the  $\text{Ne I}$  point is atypical of the general behavior of the sequence. As has been noted earlier [16], the mixing angle for  $\text{Ne I}$  is larger than that of either  $\text{Na II}$  or  $\text{Mg III}$ , an effect that occurs in conjunction with a strong contraction of the  $3s$  orbital that occurs between  $\text{Ne I}$  and  $\text{Na II}$  [74]. This could result in a coupling condition anomaly for  $\text{Ne I}$ , which could cause the mixing angle parametrizations for the energy levels and the line strengths to differ. Such an anomaly would affect the reduced intercombination line strength much more strongly

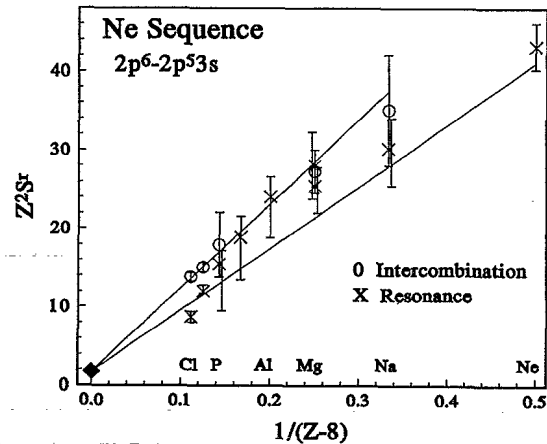


FIG. 3. Plot of charge-scaled reduced line strengths vs the reciprocal screened charge for the  $2p^6-2p^5 3s$  transitions in the Ne isoelectronic sequence. Measured values are denoted by  $\circ$  for the intercombination transition and by  $\times$  for the resonance transition. The high- $Z$  hydrogenlike limit is denoted by  $\diamond$  and the solid lines trace weighted least-squares fits.

than the reduced resonance transition line strength because  $\sin^2 \vartheta$  is more rapidly varying than  $\cos^2 \vartheta$  for small values of  $\vartheta$ .

## VII. CONCLUSIONS

The results presented here indicate that the predictive regularities revealed earlier for  $\Delta n = 0$  transitions persist for  $\Delta n = 1$  transitions. Moreover, the trends confirm the suggestion that an interpolation can be made to a precisely known high- $Z$  limit given by a hydrogenlike calculation. Predicted values for transition probabilities are presented and the accuracy of this approach can be tested and the predictions sharpened through subsequent measurements.

## ACKNOWLEDGMENT

This work was supported by the U.S. Department of Energy, Office of Basic Energy Sciences, Division of Chemical Sciences, under Grant No. DE-FG05-88ER13958.

[1] L. J. Curtis, *Phys. Rev. A* **40**, 6958 (1989).  
 [2] L. J. Curtis, *Phys. Scr.* **43**, 137 (1991).  
 [3] L. J. Curtis, *J. Opt. Soc. Am. B* **9**, 5 (1992).  
 [4] E. Träbert and L. J. Curtis, *Phys. Scr.* **48**, 586 (1993).  
 [5] L. J. Curtis, *J. Phys. B* **26**, L589 (1993).  
 [6] L. J. Curtis and D. G. Ellis, *J. Phys. B* **11**, L543 (1978).  
 [7] L. J. Curtis, D. G. Ellis, and I. Martinson, *Phys. Rev. A* **51**, 251 (1995).  
 [8] S. M. Younger and A. W. Weiss, *J. Res. Natl. Bur. Stand. Sect. A* **79**, 629 (1975).  
 [9] J. Linderberg and H. Shull, *J. Mol. Spectrosc.* **5**, 1 (1960).  
 [10] R. R. Haar, D. J. Beideck, L. J. Curtis, T. J. Kvale,

A. Sen, R. M. Schectman, and H. W. Stevens, *Nucl. Instrum. Methods Phys. Res. Sect. B* **79**, 746 (1993).  
 [11] E. Träbert, P. H. Heckmann, J. Doerfert, and J. Granzow, *J. Phys. B* **25**, L353 (1992).  
 [12] J. H. Blanke, P. H. Heckmann, E. Träbert, R. Hucke, and H. v. Buttler, *Z. Phys. A* **321**, 47 (1985).  
 [13] L. Engström and K. Håkansson, *Phys. Scr.* **43**, 475 (1991).  
 [14] L. Engström and P. Bengtsson, *Phys. Scr.* **43**, 480 (1991).  
 [15] S. T. Maniak and L. J. Curtis, *Phys. Rev. A* **42**, 1821 (1990).  
 [16] R. D. Cowan, *The Theory of Atomic Structure and Spec-*

- tra* (University of California Press, Berkeley, 1981), pp. 295-297.
- [17] L.J. Curtis, *J. Phys. B* **25**, 1427 (1992).
- [18] L. Johansson, *Ark. Fys.* **23**, 119 (1962).
- [19] A. Ölme, *Phys. Scr.* **1**, 256 (1970).
- [20] K. Bockasten, *Ark. Fys.* **9**, 457 (1955).
- [21] R. Hallin, *Ark. Fys.* **32**, 201 (1966).
- [22] K. Bockasten and K. B. Johansson, *Ark. Fys.* **38**, 563 (1968).
- [23] L. Engström, *Phys. Scr.* **31**, 379 (1985).
- [24] K. Bockasten, R. Hallin, and T. P. Hughes, *Proc. Phys. Soc.* **81**, 522 (1963).
- [25] D. G. Ellis, *Phys. Rev. A* **28**, 1223 (1983).
- [26] Y.-K. Kim, W. C. Martin, and A. W. Weiss, *J. Opt. Soc. Am. B* **5**, 2215 (1988).
- [27] L. Engström, B. Denne, S. Huldt, J. O. Ekberg, L. J. Curtis, E. Veje, and I. Martinson, *Phys. Scr.* **20**, 88 (1979).
- [28] J. E. Hardis, L. J. Curtis, P. S. Ramanujam, A. E. Livingston, and R. L. Brooks, *Phys. Rev. A* **27**, 257 (1983).
- [29] J. Granzow, P. H. Heckmann, and E. Träbert, *Phys. Scr.* **49**, 148 (1994).
- [30] E. Fritzsche and I. P. Grant, *Phys. Scr.* **50**, 473 (1994).
- [31] A. Hibbert, *J. Phys. B* **12**, L661 (1979).
- [32] H. Nussbaumer, *Astron. Astrophys.* **16**, 77 (1972).
- [33] D. H. Sampson, R. E. H. Clark, and E. J. Goett, *Phys. Rev. A* **24**, 2979 (1981).
- [34] J. A. Kernahan, E. H. Pinnington, A. E. Livingston, and D. J. G. Irwin, *Phys. Scr.* **12**, 319 (1975).
- [35] I. Martinson, W. S. Bickel, and A. Ölme, *J. Opt. Soc. Am.* **9**, 1213 (1970).
- [36] T. Andersen, K. A. Jessen, and G. Sørensen, *Phys. Rev. A* **188**, 76 (1969).
- [37] M. C. Buchet-Poulizac and J. P. Buchet, *Phys. Scr.* **8**, 40 (1973).
- [38] D. Dumont, Y. Baudinet-Robinet, and A. E. Livingston, *Phys. Scr.* **13**, 365 (1976).
- [39] E. J. Knystautas and R. Drouin, *J. Phys. B* **8**, 2001 (1975).
- [40] C. Laughlin, E. R. Constantinides, and G. A. Victor, *J. Phys. B* **11**, 2243 (1978).
- [41] A. K. Bhatia and H. E. Mason, *Astron. Astrophys.* **103**, 324 (1981).
- [42] L. J. Curtis, *Phys. Scr.* **48**, 559 (1993).
- [43] M. D. Rosen, P. L. Hagelstein, D. L. Matthews, E. M. Campbell, A. U. Hazi, B. L. Whitten, B. MacGowan, R. E. Turner, R. W. Lee, G. Charatis, G. E. Busch, C. E. Shepard, and P. D. Rockett, *Phys. Rev. Lett.* **54**, 106 (1985).
- [44] D. L. Matthews, P. L. Hagelstein, M. D. Rosen, M. J. Eckart, N. M. Ceglio, A. U. Hazi, H. Medeck, B. J. MacGowan, J. E. Trebes, B. L. Whitten, E. M. Campbell, C. W. Hatcher, A. M. Hawryluk, R. L. Kauffman, L. D. Pleasance, G. Rambach, J. H. Scofield, G. Stone, and T. A. Weaver, *Phys. Rev. Lett.* **54**, 110 (1985).
- [45] B. Edlén, in *Atomic Energy Levels*, Natl. Bur. Stand. Ref. Data Ser., Natl. Bur. Stand. (U.S.) Circ. No. 35, edited by C. E. Moore (U.S. G. P. Office, Washington, DC, 1948).
- [46] W. C. Martin and R. Zuluaba, *J. Phys. Chem. Ref. Data* **10**, 153 (1981); **9**, 1 (1980); **8**, 817 (1979); **12**, 323 (1983).
- [47] M. Eidelsberg and M.-C. Artru, *Phys. Scr.* **16**, 109 (1977).
- [48] C. Jupén (private communication).
- [49] C. Jupén, *Phys. Scr.* **36**, 776 (1987).
- [50] L. Engström and H. G. Berry, *Phys. Scr.* **34**, 131 (1986).
- [51] R. R. Gayazov, A. E. Kramida, L. I. Podobedova, E. N. Ragozin, and V. A. Chirkov, in *X-Ray Plasma Spectroscopy and Properties of Multiply Charged Ions*, edited by I. I. Sobelman (Nova Science, Moscow, 1988), pp. 79-114.
- [52] C. Jupén, U. Litzén, V. Kaufman, and J. Sugar, *Phys. Rev. A* **35**, 116 (1987).
- [53] J. P. Buchet, M. C. Buchet-Poulizac, A. Denis, J. Désesquelles, M. Druetta, S. Martin, and J.-F. Wyart, *J. Phys. B* **20**, 1709 (1987).
- [54] E. P. Ivanova and A. V. Glushkov, *J. Quant. Spectrosc. Radiat. Transfer* **36**, 127 (1986).
- [55] P. Quinet, T. Gorlia, and E. Biémont, *Phys. Scr.* **44**, 164 (1991).
- [56] G. M. Lawrence and H. S. Liszt, *Phys. Rev.* **178**, 122 (1969).
- [57] J. A. Kernahan, A. Denis, and R. Drouin, *Phys. Scr.* **4**, 49 (1971).
- [58] W. Schlagheck, *Phys. Lett.* **54A**, 181 (1975).
- [59] W. Schlagheck, Doctoral dissertation, Ruhr-Universität Bochum, 1975 (unpublished).
- [60] J. P. Buchet, M. C. Buchet-Poulizac, and P. Ceyzeriat, *Phys. Lett. A* **77**, 424 (1980).
- [61] M. Westerlind, L. Engström, P. Bengtsson, and L. J. Curtis, *Phys. Rev. A* **45**, 6198 (1992).
- [62] R. K. Gardner, C. L. Cocke, T. K. Saylor, and B. Curnutte, *J. Opt. Soc. Am.* **68**, 830 (1978).
- [63] H. G. Berry, J. Désesquelles, K. T. Cheng, and R. M. Schectman, *Phys. Rev. A* **8**, 546 (1978).
- [64] L. J. Curtis, in *Beam-Foil Spectroscopy*, edited by S. Bashkin (Springer, Berlin, 1976), pp. 63-109.
- [65] M. Kirm, P. Bengtsson, and L. Engström (unpublished).
- [66] A. Hibbert, M. Mohan, and M. LeDourneuf, *J. Phys. B* **25**, 1107 (1992).
- [67] M. Westerlind, L. Engström, R. Hutton, N. Reistad, S. Bliman, M. Raphaelian, and H. G. Berry, *Phys. Scr.* **38**, 821 (1988).
- [68] L. Engström, *J. Phys. B* **24**, 5077 (1991).
- [69] A. Hibbert, M. LeDourneuf, and M. Mohan, *At. Data Nucl. Data Tables* **53**, 23 (1993).
- [70] L. LaJohn, *Phys. Scr.* **49**, 169 (1994).
- [71] M. Crance, *At. Data* **5**, 186 (1973).
- [72] L. A. Bureeva and V. I. Safronova, *Phys. Scr.* **20**, 81 (1979).
- [73] E. Biémont and J. E. Hansen, *At. Data Nucl. Data Tables* **37**, 1 (1987).
- [74] R. D. Cowan (private communication).